Journal of Applied Mechanics and Technical Physics, Vol. 40, No. 1, 1999

EXPERIMENTAL AND NUMERICAL STUDY OF THE STABILITY OF A PRE-SEPARATED FLOW ON AN AIRFOIL

N. D. Dikovskaya and B. Yu. Zanin

UDC 532.516

The problem of the origin and evolution of two-dimensional waves of unstable disturbances in the boundary layer on an airfoil in the region of adverse pressure gradient in the pre-separation flow region is solved numerically. The stability of the experimental velocity profiles, including the inflected profiles, is studied. As a result of the calculations, the boundaries of the instability region and the parameters of the maximally unstable disturbances (frequency, growth rate, wavelength, and propagation velocity) are determined for each velocity profile. The characteristics obtained in the present work are in good agreement with the real experimental parameters of instability waves.

Introduction. Studies of the origin of turbulence on an airfoil under flight and model conditions [1, 2] showed that the transition from laminar to turbulent flow in the boundary layer occurs as a result of the appearance, development, and destruction of a packet of instability waves in the region of adverse pressure gradient in the tail part of the airfoil. The mean-velocity profiles in the boundary layer in this part of the airfoil acquire a shape with an inflection point, and further downstream the separation of the laminar boundary layer with subsequent turbulent reattachment occurs, i.e., a laminar separation bubble is formed on the airfoil. The appearance of a discrete wave packet in a pre-separated flow was also observed in other experiments [3, 4]. However, it is rather difficult to study experimentally the initial stages of the evolution of perturbations, since the disturbance amplitudes are smaller than the level of background fluctuations in the boundary layer and hot-wire measurements do not yield the necessary information. Therefore, the objective of the present work was to calculate the evolution of disturbances at the early stage of development, which is unavailable for experimental observation. To study the initial stage of the origin of turbulence in the boundary layer, the stability of the experimentally measured mean-velocity profiles was analyzed numerically. The numerical studies should answer the following questions: at which place in the boundary layer the packet of instability waves appears for the first time and how the changes in the shape of the mean-velocity profiles affect the characteristics of flow stability when the separation point is reached. The results obtained were compared with experimental [2] and numerical [5–7] data on the evolution of instability waves.

1. Experimental Data. The experiment [2] was conducted in a T-324 low-turbulent wind tunnel of the Institute of Theoretical and Applied Mechanics (ITAM) of the Siberian Division of the Russian Academy of Sciences, which has a level of flow turbulence lower than 0.04%, on an airfoil with an NACA profile and a mean chord $b = 270$ mm. The results used in calculations were obtained for an angle of attack of the model of 4° and a free-stream velocity $U_0 = 25$ m/sec. Figure 1 shows the distributions of the static-pressure coefficient C_p (the solid curve) and the longitudinal static-pressure gradient dC_p/dX (the dashed curve) along the chord of the model (a), the profiles of the longitudinal component of the mean velocity $U(y)$ in the boundary layer in different cross sections $X = x/b = 0.19$–0.59 (b), and the frequency spectra of fluctuations at the line of equal mean velocities $U = 0.5U_0$ (c).

Institute of Theoretical and Applied Mechanics, Siberian Division, Russian Academy of Sciences, Novosibirsk 630090. Translated from Prikladnaya Mekhanika i Tekhnicheskaya Fizika, Vol. 40, No. 1, pp. 126–132, January–February, 1999. Original article submitted April 18, 1997.

 0021-8944/99/4001-0108 $22.00

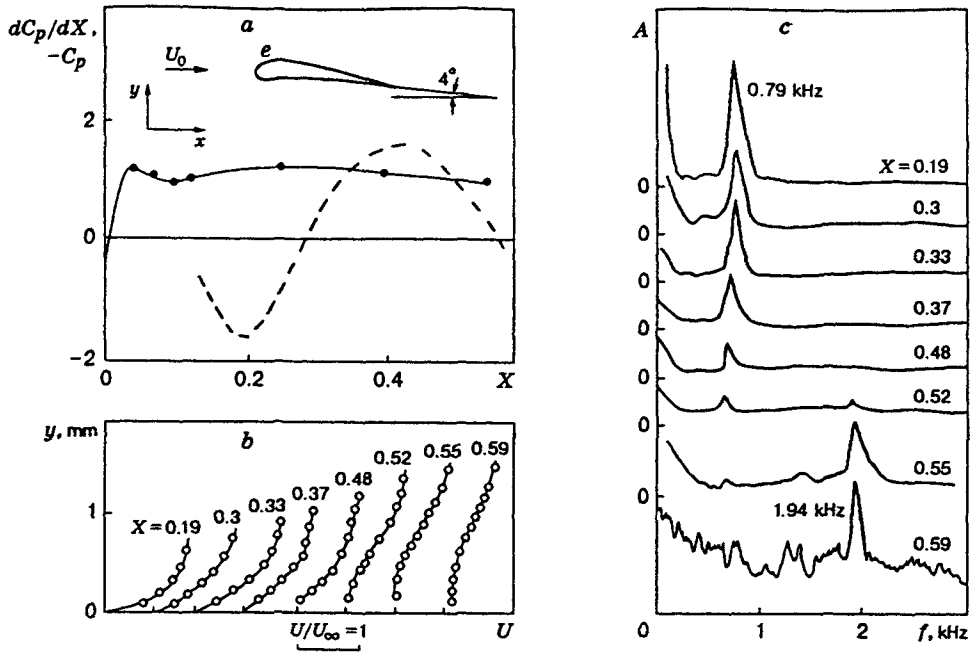

Fig. 1

The static-pressure measurements show that there are two local minima in the pressure distribution on the model surface and, hence, two regions with adverse pressure gradient: near the leading edge and in the tail part of the model ($X > 0.3$). In each of these regions, an individual packet of instability waves appears and develops, which is evidenced by the frequency spectra of fluctuations (Fig. 1c). The appearance of the first wave packet with a frequency of 0.79 kHz is apparently caused by the presence of a small region of adverse pressure gradient in the nose part of the airfoil. The wave formed here degrades, and this degradation continues when this wave enters the second region of adverse pressure gradient, where its own packet of instability waves with a frequency of 1.94 kHz appears and develops. The amplification of the latter wave packet leads to the transition. This wave packet appears in the frequency spectra only at $X = 0.52$, where its amplitude becomes greater than the amplitude of background fluctuations in the boundary layer.

The measurements show (Fig. 1b) that an inflection point appears in the mean-velocity profiles $U(y)$ in the region of adverse pressure gradient ($X > 0.3$); hence, the flow acquires inviscid instability in addition to viscous instability. The laminar form of the boundary-layer flow remains up to the cross section $X = 0.55$, where the velocity fluctuations do not exceed 1%. The mean-velocity profiles gradually acquire a pre-separated shape, but the flow remains attached until the cross section $X = 0.52$. An analysis of the stability of experimentally measured mean-velocity profiles is given below.

2. Calculation of Stability. The stability of a laminar boundary layer developing under the conditions of gradient flow was calculated within the framework of the linear theory of the growth of small perturbations under the assumption of "local parallelism" of two-dimensional flow. Two-dimensional disturbances were considered, which are fluctuations periodic in time $(u, v) = [u^0(y), v^0(y)] \exp[i(\alpha x - \omega t)]$. Here $\alpha = \alpha_r + i\alpha_i$ (α_r is the wavenumber and α_i is the spatial growth rate of the disturbance) and $\omega = 2\pi f$ is the angular frequency of the wave. For $\alpha_i > 0$, the perturbations propagating in the streamwise direction degrade, and the flow is stable. For $\alpha_i < 0$, the perturbations increase, i.e., the flow is unstable.

We solved the eigenvalue problem for the Orr–Sommerfeld equation written for the perturbation amplitudes $v^0(y)$ (in what follows, the superscript 0 is omitted for simplicity):

$$(v'' - \alpha^2 v)'' - [\alpha^2 + i\,\mathrm{Re}\,(\alpha U - \omega)](v'' - \alpha^2 v) + i\alpha \mathrm{Re}\, U'' v = 0. \qquad (2.1)$$

Here $(\,)' = d(\,)/dy$ and U is the main-flow velocity in the boundary layer with the boundary conditions of decaying perturbations on the wall and in the external flow: $v(0) = v'(0) = 0$ for $y = 0$ and $v(y) = v'(y) = 0$ for $y \to \infty$.

All quantities in Eq. (2.1) are normalized to the velocity U_e at the boundary-layer edge and to the complex $(\delta_1/1.72)$. Here $\mathrm{Re} = U_e(\delta_1/1.72)/\nu$ is the Reynolds number, $F = 2\pi f\nu/U_e^2$ is the frequency parameter, ν is the kinematic viscosity, $\omega = F \cdot \mathrm{Re}$ is the dimensionless frequency, $c_r = \omega/\alpha_r$ is the phase velocity of wave propagation along the flow, and δ_1 is the displacement thickness. The amplitude of the longitudinal component of velocity fluctuations was found from the relationship $u(y) = v'/(-i\alpha_i)$.

In solving Eq. (2.1), we used the fourth-order Runge–Kutta method for differential equations, orthogonalization methods, and the method of iterations; the iterations were conducted using the Newton method. In most cases, the eigenvalues were determined to an accuracy of 10^{-5}.

We assumed that the dependence $U(y)$ near the surface is described by the trinomial

$$U(y) = a_1 + a_2 y + a_3 y^2. \tag{2.2}$$

The last term is introduced into Eq. (2.2) because of the pressure gradient at the outer edge of the boundary layer. According to [8], we have

$$\frac{dC_p}{dX} = \frac{kd^2U}{dy^2}, \tag{2.3}$$

where k is a coefficient that depends on the method of normalization of the entering quantities. It follows from Eqs. (2.2) and (2.3) that $d^2U/dy^2 = 2a_3$ and $dC_p/dX = 2a_3k$, where $a_3 = (1/2k)\,dC_p/dX \neq 0$. The coefficients a_1 and a_2 were found from the known values of velocity at two measurement points nearest to the surface. Then the allowance y^* from the condition $U(y^*) = 0$ was introduced to correct the systematic experimental error caused by the difficulties in measurement of the small quantities y and U. For all profiles $U(y)$ considered, the value of y^* did not exceed 0.08 mm. In some cases, we had to vary the value of U at the measurement point nearest to the surface within the experimental uncertainty to satisfy condition (2.3). The thus-supplemented profiles $U(y)$ were smoothed using polynomials of power $n = 5$ and $n = 6$, which allowed us to satisfy the requirements of smoothness of the functions $U(y)$, $U'(y)$, and $U''(y)$.

3. Calculation Results. The calculation of the evolution of perturbations in the boundary layer along the airfoil chord in the range $X = 0.15$–0.52 shows that the flow is stable to all perturbation frequencies only in two first cross sections $X = 0.15$ and $X = 0.22$ located in the region of favorable pressure gradient (Fig. 1a).

Figure 2a shows the spatial growth rate of the perturbations in the dimensional form $\alpha_i(f)$ for the cross sections $X = 0.22$, 0.3, 0.37, 0.44, and 0.52 (curves 1–5, respectively). It follows that the flow is stable and there are no increasing perturbations in the cross section $X = 0.22$ (in the region of favorable pressure gradient). In the cross section $X = 0.3$ located in the beginning of the region of adverse pressure gradient, the peak value of the spatial growth rate $(-\alpha_i)_m$, which is at the frequency $f_m = 1.8$–1.9 kHz, is close to zero. Taking into account the difficulties in measurement of the experimental velocity profile, and also the strong dependence of α_i on the method of approximation and the rather stable value of f_m (see [9]), we can assume that the first increasing perturbation frequency is located in the cross section $X = 0.3$. Further downstream, the range of unstable frequencies Δf expands, and the spatial growth rate $-\alpha_i$ increases by three orders of magnitude over the length from $X = 0.37$ to $X = 0.52$.

Figure 2b shows the calculated Strouhal numbers $\mathrm{Sr} = f\delta_2/U_e$ for the neutral (curves 1 and 2) and maximally increasing perturbations (curve 3), and also the phase velocity c_r of propagation of perturbations corresponding to the second branch of the neutral stability curve (curve 4) and the velocity U_i at the inflection point (curve 5) in each cross section. The value of Sr for the maximally growing frequencies remains almost constant and equal to 0.0068 for all cross sections, except for the last one ($X = 0.52$) in which the Strouhal number increases to 0.01. The range of unstable frequencies gradually expands due to the involvement of both high and low frequencies down to zero values of ω at $X = 0.52$. The amplification of perturbations in the low-frequency range is typical of free shear flows [7] wherein the inviscid instability is determining. It was in this cross section that a peak at the frequency $f_0 = 1.94$ kHz was experimentally registered for the first time (see Fig. 1c). The Strouhal number $\mathrm{Sr}_0 = 0.012$ corresponding to this frequency and marked by diamonds in Fig. 2b demonstrates good agreement between the calculated and experimental data.

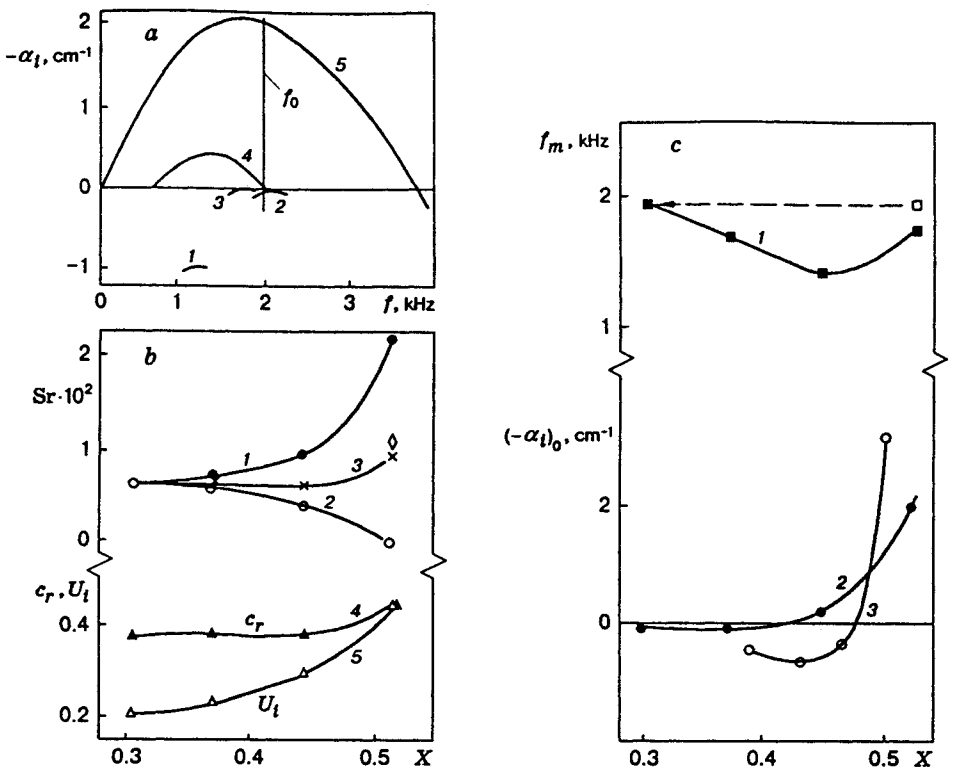

Fig. 2

The contribution of inviscid instability in the cross section $X = 0.52$ can be evaluated from the Strouhal number $\mathrm{Sr}^* = f\delta_2/U^*$ calculated from the mean shear velocity $U^* = U_e/2$, as is done for mixing layers, for zero velocity of one of the flows. The resultant value $\mathrm{Sr}^* = 0.022$ corresponds to the growth rate of perturbations for the free shear flow, which is roughly equal to 75% of the maximum value [7]. This indicates that inviscid instability plays an important, though not an exclusive role in the cross section considered.

Muti Lin and Pauly [6] simulated numerically a similar flow and obtained $\mathrm{Sr} = 0.0066$. They associate this frequency with the shedding of vortices which arise in the beginning of the laminar separation bubble. However, it follows from our calculations that the maximally growing frequency f_m, which corresponds to the peak in the perturbation spectra observed experimentally (see Fig. 1c), exists prior to flow separation, i.e., in an attached boundary layer.

At the early stage of evolution of the perturbations, the velocity U_i at the inflection point (curve 5 in Fig. 2b) is substantially smaller than the phase velocity c_r of propagation of the perturbations that correspond to the second branch of the neutral stability curve (curve 4 in Fig. 2b), which coincides with the calculation results [5]. Further downstream, as the inflection point moves away from the surface, the velocity U_i increases and coincides with the corresponding value of c_r in the cross section $X = 0.52$, i.e., according to [7], the main mechanism of evolution of the perturbations in this cross section is the inviscid instability.

Thus, we can see from Fig. 2b that viscous instability exists together with inviscid instability on the airfoil in the region of adverse pressure gradient for profiles with an inflection point. Moreover, viscous instability plays a dominant role in the beginning of this region until the cross section $X = 0.44$. Further downstream, in the cross section $X = 0.52$, the governing mechanism of evolution of the perturbations is the inviscid instability, though the viscous instability is still present.

The results obtained allow us to find the point of appearance of perturbations with the frequency $f_0 = 1.94$ kHz, which were observed experimentally in the cross section $X = 0.52$, and trace the regularities of their development in the region unavailable for experimental observation (upstream to $X = 0.52$). The calculated frequencies f_m of the maximally increasing perturbations versus the X coordinate are shown in

Fig. 2c (curve 1) in comparison with the experimental value of f_0 (the point □). The calculated (curve 2) and experimental (curve 3) spatial growth rates $(-\alpha_i)_0$ of the perturbations at the frequency f_0 are also plotted here.

It can be seen that increasing perturbations with the central frequency equal to $f_m = 1.8$–1.9 kHz, i.e., corresponding to the value of f_0, appear in the boundary layer in the beginning of the flow deceleration region (near $X = 0.3$). Further downstream, the frequency f_0 is outside the amplification region, i.e., under stabilizing conditions, and its growth rate is $(-\alpha_i)_0 < 0$. Still further downstream, in the cross section $X = 0.52$ with a wide range of unstable frequencies and a rather flat maximum in the dependence $\alpha_i(f)$, the perturbations with the frequency f_0 enter the region with rather high growth rates $(-\alpha_i)_0 > 0$ and rapidly increase. The behavior of the calculated and experimental curves $(-\alpha_i)_0$ versus X are in good qualitative agreement.

Thus, the peak frequency $f_0 = 1.94$ kHz, which was observed experimentally at $X = 0.52$ for the first time, is close to the calculated maximally increasing frequency $f_m = 1.8$–1.9 kHz for the cross section located much more upstream, in the beginning of the region of adverse pressure gradient ($X = 0.3$).

In addition, the calculations show that in the region of viscous instability the wavelength λ of the maximally increasing perturbations that arise in this cross section depends on the local boundary-layer thickness δ, which is described by the formula $\lambda = 2\pi\delta$ proposed by Zanin [2].

Conclusions. The stability of the laminar boundary layer has been calculated. The calculation is based on the measured mean-velocity profiles on an airfoil. The characteristics of evolution of the perturbations in the boundary layer at the early stage of their development, which is unavailable for experimental observation, have been determined. It is shown that unstable perturbations appear for the first time in the beginning of the region of adverse pressure gradient. Further downstream, the region of unstable frequencies expands, but the dimensionless maximally increasing frequency ω_m and the corresponding Strouhal numbers change little as long as the velocity at the inflection point is smaller than the propagation velocity of the perturbations. In this region, viscous instability is realized even in the presence of an inflection point in the mean-velocity profiles. Further downstream, when the velocity at the inflection point reaches the value of the perturbation propagation velocity, the governing mechanism of evolution of the perturbations becomes the inviscid instability, and a rapid increase in the amplitude of fluctuations is observed.

The central frequency f_0 of the wave packet observed in the frequency spectra in the pre-separated flow is determined by the boundary-layer characteristics in the upstream cross section, namely, by the beginning of the region of adverse pressure gradient.

Good qualitative agreement between the variation of the growth rate of perturbations $(-\alpha_i)_0$ along the chord and the frequency f_0 obtained in the calculation and observed in the experiments is noted.

The authors are grateful to Dr. A. Hanifi from the Royal Institute of Technology (Stockholm, Sweden) for the kindly granted code for calculating the stability of the subsonic two-dimensional boundary layer [10]. We adapted the code and made some changes, which allowed us, in particular, to calculate the stability of the mean-velocity profiles measured experimentally.

This work was supported by the Russian Foundation for Fundamental Research (Grant Nos. 96-15-96310 and 97-01-00821).

REFERENCES

1. B. Yu. Zanin and V. V. Kozlov, "In-flight studies of the boundary-layer structure," *Uch. Zap. TsAGI*, **14**, No. 6, 109–112 (1983).
2. B. Yu. Zanin, "Parameters of wave instability in a boundary layer," *Inzh.-Fiz. Zh.*, **53**, No. 4, 624–629 (1987).
3. A. V. Boiko, A. V. Dovgal', and V. V. Kozlov, "Nonlinear interactions of perturbations during the transition to turbulence in the region of separation of a laminar boundary layer," *Izv. Sib. Otd. Akad. Nauk SSSR, Ser. Tekh. Nauk*, No. 18, Issue 5, 44–49 (1988).

4. P. Leblanc, R. Blackwelder, and R. Liebeck, "Experimental results of laminar separation on two airfoils at low Reynolds numbers," in: Rep. on 29th Aerospace Sci. Meeting, Reno, Nevada (1991), pp. 1–14.
5. V. M. Galkin, B. Yu. Zanin, and V. A. Kuparev, "Calculation of the parameters of instability waves in the pre-separation region," *Sib. Fiz.-Tekh. Zh.*, No. 2, 25–28 (1993).
6. J. C. Muti Lin and L. L. Pauly, "Low-Reynolds-number separation on an airfoil," *AIAA J.*, **34**, No. 8, 1570–1577 (1996).
7. P. A. Monkewitz and P. Huerre, "The influence of the velocity ratio on the spatial instability of mixing layers," *Phys. Fluids*, **25**, 1137–1143 (1982).
8. G. Schlichting, *Boundary Layer Theory*, McGraw-Hill, New York (1968).
9. N. D. Dikovskaya and B. Yu. Zanin, "Verification of the stability calculation of the boundary layer flow on the wing profile," in: *Proc. 8th Int. Conf. on the Methods of Aerophys. Research*, Part 2, Novosibirsk (1996), pp. 58–63.
10. A. Hanifi, "Stability characteristics of the supersonic boundary layer on a yawed cone," in: Licentiate Thesis, TRITA-MEK, Techn. Rep. No. 6, Royal Inst. of Technol., Stockholm (1993).